The Journal of Pathology: Clinical Research
J Pathol Clin Res March 2022; **8:** 155–168
Published online 17 November 2021 in Wiley Online Library (wileyonlinelibrary.com). DOI: 10.1002/cjp2.247

ORIGINAL ARTICLE

Papillary thyroid carcinoma tall cell variant shares accumulation of mitochondria, mitochondrial DNA mutations, and loss of oxidative phosphorylation complex I integrity with oncocytic tumors

Oleksiy Tsybrovskyy[1,2†*], Monica De Luise[3†], Dario de Biase[4], Leonardo Caporali[5], Claudio Fiorini[5], Giuseppe Gasparre[3], Valerio Carelli[5,6], Dominik Hackl[7], Larisa Imamovic[8], Silke Haim[8], Manuel Sobrinho-Simões[9‡] and Giovanni Tallini[10‡*]

[1]*Diagnostic and Research Institute of Pathology, Medical University of Graz, Graz, Austria*
[2]*Department of Clinical Pathology, Ordensklinikum/Hospital of the Sisters of Charity, Linz, Austria*
[3]*Department of Medical and Surgical Sciences (DIMEC) and Center for Applied Biomedical Research (CRBA), University of Bologna, Bologna, Italy*
[4]*Department of Pharmacy and Biotechnology (FABIT), University of Bologna, Bologna, Italy*
[5]*Programma di Neurogenetica, IRCCS Istituto delle Scienze Neurologiche, Bologna, Italy*
[6]*Department of Biomedical and Neuromotor Sciences (DIBINEM), University of Bologna, Bologna, Italy*
[7]*Department of General and Visceral Surgery, Ordensklinikum/Hospital of the Sisters of Charity, Linz, Austria*
[8]*Department of Nuclear Medicine & Endocrinology, PET-CT Center Linz, Ordensklinikum/Hospital of the Sisters of Charity, Linz, Austria*
[9]*Ipatimup, Institute of Molecular Pathology and Immunology of the University of Porto, Porto, Portugal*
[10]*Department of Experimental, Diagnostic and Specialty Medicine (DIMES), University of Bologna, Bologna, Italy*

**Correspondence to: Giovanni Tallini, Department of Experimental, Diagnostic and Specialty Medicine (DIMES), University of Bologna, Pathology Unit, Istituto Oncologico "F.Addarii" – Policlinico di S. Orsola Viale Ercolani 4/2, 40138 Bologna, Italy. E-mail: giovanni.tallini@unibo.it; and Oleksiy Tsybrovskyy, Diagnostic and Research Institute of Pathology, Medical University of Graz, Neue Stiftingtalstrasse 6, 8010 Graz, Austria. E-mail: o.tsybrovskyy@medunigraz.at*

[†]*Share junior authorship.*
[‡]*Share senior authorship.*

Abstract

Papillary thyroid carcinoma tall cell variant (PTC-TCV), a form of PTC regarded as an aggressive subtype, shares several morphologic features with oncocytic tumors. Pathogenic homoplasmic/highly heteroplasmic somatic mitochondrial DNA (mtDNA) mutations, usually affecting oxidative phosphorylation (OXPHOS) complex I subunits, are hallmarks of oncocytic cells. To clarify the relationship between PTC-TCV and oncocytic thyroid tumors, 17 PTC-TCV and 16 PTC non-TCV controls (cPTC) were subjected to: (1) transmission electron microscopy (TEM) to assess mitochondria accumulation, (2) next-generation sequencing to analyze mtDNA and nuclear genes frequently mutated in thyroid carcinoma, and (3) immunohistochemistry (IHC) for prohibitin and complex I subunit NDUFS4 to evaluate OXPHOS integrity. TEM showed replacement of cytoplasm by mitochondria in PTC-TCV but not in cPTC cells. All 17 PTC-TCV had at least one mtDNA mutation, totaling 21 mutations; 3/16 cPTC (19%) had mtDNA mutations ($p < 0.001$). PTC-TCV mtDNA mutations were homoplasmic/highly heteroplasmic, 16/21 (76%) mapping within mtDNA-encoded complex I subunits. MtDNA mutations in cPTC were homoplasmic in 2 cases and at low heteroplasmy in the third case, 2/3 mapping to mtDNA-encoded complex I subunits; 2/3 cPTC with mtDNA mutations had small tall cell subpopulations. PTC-TCV showed strong prohibitin expression and cPTC low-level expression, consistent with massive and limited mitochondrial content, respectively. All 17 PTC-TCV showed NDUFS4 loss (partial or complete) and 3 of 16 cPTC (19%) had (partial) NDUFS4 loss, consistent with lack of complex I integrity in PTC-TCV ($p < 0.001$). IHC loss of NDUFS4 was associated with mtDNA mutations ($p < 0.001$). Four *BRAF* V600E mutated PTCs had loss of NDUSF4 expression limited to neoplastic cell subpopulations with tall cell features, indicating that PTCs first acquire *BRAF* V600E and then mtDNA mutations. Similar to oncocytic thyroid tumors, PTC-TCV is characterized by mtDNA mutations, massive accumulation of mitochondria, and loss of OXPHOS integrity. IHC loss of NDUFS-4 can be used as a surrogate marker for OXPHOS disruption and to reliably diagnose PTC-TCV.

Keywords: mitochondria; mitochondrial DNA mutations; papillary thyroid carcinoma; tall cell variant papillary carcinoma; *BRAF* V600E; oncocytic tumors; thyroid tumor diagnosis

Received 1 August 2021; Revised 14 September 2021; Accepted 27 September 2021

No conflicts of interest were declared.

Introduction

Papillary thyroid carcinoma (PTC) tall cell variant (PTC-TCV) is composed of cells that are 'tall', i.e. they are 2–3 times taller than wide. Additional features include complex papillary formation with trabecular architecture ('tram track' pattern), older patient age, and the common occurrence of *BRAF* V600E mutations. Starting with its first description by Hawk and Hazard in 1976 [1], numerous studies repeatedly found PTC-TCV to be associated with aggressive clinical features and reduced patient survival [2–9], and it has long been debated whether the tall cell features represent an independent prognostic factor for PTC [10–18]. Current American Thyroid Association (ATA) and European Society for Medical Oncology (ESMO) guidelines regard PTC-TCV as a variant with 'aggressive histology' [19,20]. Accordingly, patients with PTC-TCV are considered at least intermediate-risk and are managed more aggressively in terms of both surgery and adjuvant radioactive iodine (RAI) administration. Thus, it is important to correctly recognize PTC-TCV but, unfortunately, its diagnosis is rather inconsistent among pathologists (even at the expert level) [21]. Causes of the discrepancies are the subjective nature of the interpretation of morphologic criteria, their frequently non-uniform expression within the tumor, the fact that tall cell clusters are frequently present in otherwise classic papillary carcinomas, and the lack of immunohistochemical or molecular markers for PTC-TCV [12,18,21]. The tall cells of PTC-TCV have abundant 'oncocytoid' eosinophilic cytoplasm. While it is generally recognized that they are rich in mitochondria [22,23], very few electron microscopy studies have linked the abundance of mitochondria to PTC-TCV [24]. Homoplasmic/highly heteroplasmic somatic mitochondrial DNA (mtDNA) mutations that are pathogenic for the encoded molecules, and that often involve complex I subunits of the oxidative phosphorylation (OXPHOS) system, cause OXPHOS impairment leading to the accumulation of mitochondria, which defines oncocytic cells in the thyroid [25–27] as well as in other organs, including the kidney, pituitary, salivary, and parathyroid glands [28–32]. While these homoplasmic/highly heteroplasmic mutations occur in oncocytic tumors, they are also present in some papillary carcinomas [26], including those analyzed in the 2014 TCGA study [33,34].

Given this context, the aim of this study is to clarify the relationship between PTC-TCV and oncocytic thyroid carcinoma. For this purpose, we collected a series of PTCs with and without tall cell features, reviewed their histologic and clinicopathologic features, performed electron microscopy, subjected all samples to next-generation sequencing (NGS) to analyze the entire mitochondrial genome of all cases and to identify the status of those nuclear genes that are frequently mutated in thyroid carcinoma, and assessed OXPHOS complex I integrity by immunohistochemistry (IHC).

Materials and methods

Case selection

Thirty-three representative PTCs – with and without tall cell features – that belonged to 31 patients were randomly selected from the archival material of the Pathology Unit, Odrensklinikum Linz, Linz, Austria. Hematoxylin and eosin (H&E)-stained slides were reviewed by OT, GT, and MS-S and allocated to test (PTC-TCV, 17 cases) and control PTC cases (cPTC, 16 cases) following current histopathologic criteria [22] (see Supplementary materials and methods). In four cases, both primary and metastatic tissue was included; thus, a total of 37 samples were analyzed from 31 patients. The study complied with the ethics principles of the Declaration of Helsinki and followed Institutional Review Board approved protocols in Bologna, Italy, and Linz, Austria.

DNA extraction and mutation analysis of nuclear and mtDNA

Whole DNA was extracted from formalin-fixed paraffin-embedded tissue. NGS was performed with the MiSeq platform (Illumina, Inc., San Diego, CA, USA). To identify nuclear DNA mutational hot-spots for thyroid cancer genes, we used a custom-designed

NGS multigene panel [35]. The entire mtDNA was sequenced using NGS and the MitoAll re-sequencing kit (Applied Biosystems, Foster City, CA, USA), as previously described [36] (see Supplementary materials and methods for additional information).

mtDNA variant annotation

Frameshift and truncating mutations in the coding sequence dramatically alter the encoded protein and are therefore classified as pathogenic. For all other variants (synonymous, non-synonymous, noncoding intergenic variants, and variants mapping within rRNAs and tRNAs), the pathogenic potential was evaluated *in silico* with MToolBox [37], HmtVar [38], and an in-house pipeline [39] (see Supplementary materials and methods for additional information).

Electron microscopy and IHC

Transmission electron microscopy (TEM) was performed according to standard procedures. For IHC, prohibitin was used as a pan-mitochondrial marker [40], and NDUFS4 and cytochrome *c* oxidase 1 (COX-I) as markers of complex I and IV integrity, respectively [41,42]. BRAF V600E mutation-specific antibody was used to assess the distribution of the mutated protein (see Supplementary materials and methods and Table S1).

Statistical analysis

Statistical analysis was performed using the SPSS Statistics software package, version 23.0 (IBM Corp., Armonk, NY, USA). Contingency tables with exact tests (either chi-square test with Monte Carlo permutation technique or Fisher's exact test) were calculated for discrete variables. Nonparametric methods (median values and Mann–Whitney test) were used for continuous variables. For multiple comparisons, P values were obtained uncorrected and with family-wise error rate correction (Holm–Bonferroni method [43]). Differences between PTC-TCV and PTC controls and those between *BRAF* V600E mutated and *BRAF* wild-type tumors were tested separately.

Results

Clinicopathologic features

The characteristics of the patient cohort are reported in Table 1. Representative cases of one PTC-TCV and one cPTC are illustrated in Figure 1A,B. In all 17 PTC-TCV, the majority (>60%) of the tumors showed tall cell features, i.e. cell height greater than 2–3 times the cell base and long non-branching papillae resulting in trabecular architecture ('tram track' pattern) on histology sections: tall cell features represented 90% or more of the tumor in 10 of 17 PTC-TCV (supplementary material, Table S2). Fourteen cPTC cases were of classic papillary morphology. Two cPTC were unencapsulated infiltrative follicular variant PTC (Table 1).

Electron microscopy shows an accumulation of mitochondria in papillary carcinoma TCV

TEM was performed on randomly selected PTC-TCV ($n = 4$) and cPTC ($n = 4$) for which fresh tumor tissue was available for TEM processing. PTC-TCV showed massive accumulation of mitochondria, many of which were abnormally large and swollen (Figure 2). In spite of some variability, all neoplastic cells showed large sections of the cytoplasm replaced by compact clusters of mitochondria (see also Figure 1C). The cytoplasm of cPTC was largely occupied by endoplasmic reticulum and vacuoles. Mitochondria were sparse and morphologically normal (Figure 3).

BRAF V600E is the nuclear DNA mutation signature of papillary carcinoma TCV

Nuclear DNA mutations are summarized in Figure 4 and listed in supplementary material, Table S2. *BRAF* V600E was identified in all but one of the PTC-TCV using both NGS and IHC with BRAF V600E specific antibodies. In four cases, both primary tumor and lymph node metastases were analyzed (two PTC-TCV and two cPTC), and in all of them the results were concordant (Figure 4 and supplementary material, Table S2). The high *BRAF* V600E mutated allele frequencies adjusted to the proportion of neoplastic cells in the samples (supplementary material, Table S2) were consistent with the immunohistochemical findings: BRAF V600E was expressed in the vast majority of neoplastic cells within the tumor. The correlation of *BRAF* V600E with PTC-TCV, cPTC, and mitochondrial alterations (mtDNA mutation and loss of complex I integrity) is reported in Tables 2 and 3. *BRAF* V600E was statistically associated with PTC-TCV ($p = 0.002$) (Table 2) and with the mitochondrial alterations of PTC-TCV (Tables 2 and 3 and the following paragraphs).

Table 1. Clinicopathologic features of the cases analyzed.

Parameter	All cases ($n = 33^{*}$)	PTC-TCV ($n = 17$)	PTC control group ($n = 16^{\dagger}$)	Statistical significance of the difference, p
Patients' age at presentation, median (range), years	45.7 (16–81)	53.0 (28–81)	37.5 (16–66)	**0.034**
Patients' sex, female:male ratio	3.7:1	4.7:1	3.0:1	0.69
Median tumor size, maximal diameter, cm	2.5 (0.2–7.0)	2.9 (1.2–6.5)	1.8 (0.2–7.0)	0.14
Extrathyroidal tumor extension, *n* (%)				
No	16 (48%)	7 (41%)	9 (56%)	
Microscopic	15 (45%)	8 (47%)	7 (44%)	
Gross	2 (6%)	2 (12%)	0	0.49
Positive resection margins, *n* (%)				
Microscopic	6 (18%)	3 (18%)	3 (19%)	
Gross	1 (3%)	1 (6%)	0	0.62
LN metastases, *n* (%)	20/31 (65%)	10/16 (63%)	10/15 (67%)	1
Distant metastases at presentation, *n* (%)	1 (3%)	0	1 (6%)	0.49
Tumor stage (AJCC/UICC Eighth ed. 2017), *n* (%)				
Stage I	26 (79%)	12 (71%)	14 (88%)	
Stage II	7 (21%)	5 (29%)	2 (12%)	0.4
Thyroid remnant RAI ablation, *n* (%)	31 (100%)	17 (100%)	16 (100%)	1.0
Disease status at 1 year after surgery, treatment response (ATA guidelines)				
Excellent	26 (79%)	14 (82%)	12 (75%)	
Biochemical incomplete	4 (12%)	2 (12%)	2 (13%)	
Structural incomplete	1 (3%)	0	1 (6%)	
NA	2 (6%)	1 (6%)	1 (6%)	0.69
Median follow-up duration (range), months	20 (4–144)	14 (4–144)	28 (8–144)	0.37
Disease status at last follow-up, treatment response (ATA guidelines)				
Excellent	25 (76%)	14 (82%)	13 (81%)	
Biochemical incomplete	5 (15%)	1 (6%)	0	
Structural incomplete	1 (3%)	1 (6%)	2 (13%)	
NA	2 (6%)	1 (6%)	1 (6%)	0.86

Bold font indicates *P* values that are statistically significant.
AJCC, American Joint Committee on Cancer; ATA, American Thyroid Association [20]; LN, lymph node; NA: not available; UICC, Union for International Cancer Control.
[*]Two patients had two different tumors: both had one PTC-TCV and one PTC, classic type in the same thyroid gland, and both tumors were analyzed separately.
[†]The PTC control group included 14 classic PTCs and 2 infiltrative follicular variant PTCs.

Homoplasmic/highly heteroplasmic mtDNA mutations are a defining feature of papillary carcinoma TCV

The results of mtDNA analysis are summarized in Figure 4 and listed in supplementary material, Table S2. The entire mtDNA sequence was obtained in all 37 samples, of which 33 were primary tumors (17 PTC-TCV and 16 cPTC) and 4 lymph node metastases (2 from PTC-TCV and 2 from cPTC) (supplementary material, Table S2). To determine the levels of heteroplasmy, mutated allele frequencies were adjusted to the proportion of tall cells in the neoplastic area marked for analysis (supplementary material, Table S2). The results of mtDNA analysis in the four cases where both the primary tumor and lymph node metastases were analyzed (two from PTC-TCV and two from cPTC) were concordant for each sample pair (Figure 4 and supplementary material, Table S2). All 17 PTC-TCV harbored a total of 21 pathogenic mtDNA mutations, with single tumors carrying a maximum of 2 different mutations. All were at homoplasmic/highly heteroplasmic levels (supplementary material, Table S2). Sixteen of the 21 mutations (76%) identified in PTC-TCV mapped within mtDNA-encoded complex I subunits (Figure 5). Nineteen of the 21 mutations were severely pathogenic for the encoded molecule. The remaining two scored 'likely polymorphic' *in silico* by the bioinformatics tools used for mtDNA variant annotation but were associated with loss of complex I integrity (see mtDNA alterations correlate with loss of OXPHOS complex I integrity in papillary carcinoma TCV, below) (Figure 4 and supplementary material, Table S2). No mtDNA alterations were found in 13 of 16 (81%) cPTC. In each of the three remaining cPTCs, there was one mtDNA mutation per sample, pathogenic *in silico* for the encoded molecules. In two cases, there

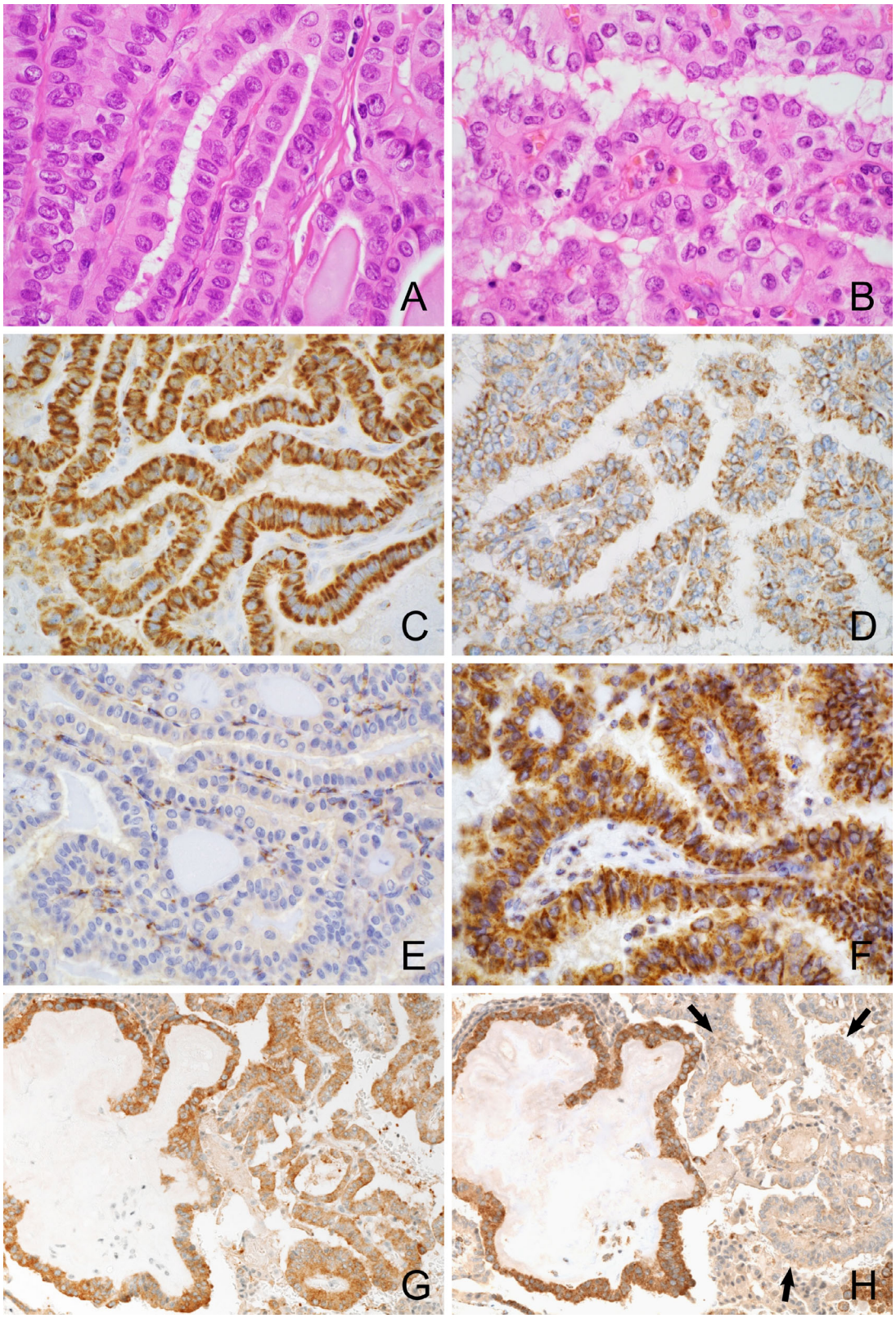

Figure 1. Legend on next page.

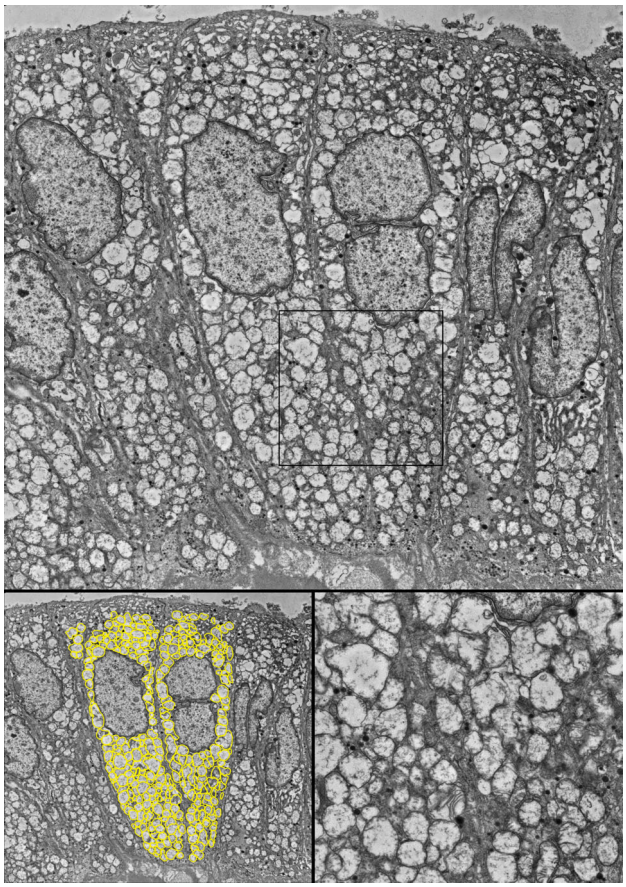

Figure 2. Cell organelle ultrastructure in PTC-TCV. Upper part: overview showing the massive accumulation of mitochondria that almost replace the entire cytoplasm of PTC-TCV cells (case T3). Lower left: same picture as above with mitochondrial mapping (yellow overlay) in two adjacent tumor cells to highlight quantity and distribution of mitochondria. Lower right: higher magnification of the inset in the upper picture demonstrates closely packed mitochondria that are enlarged and swollen.

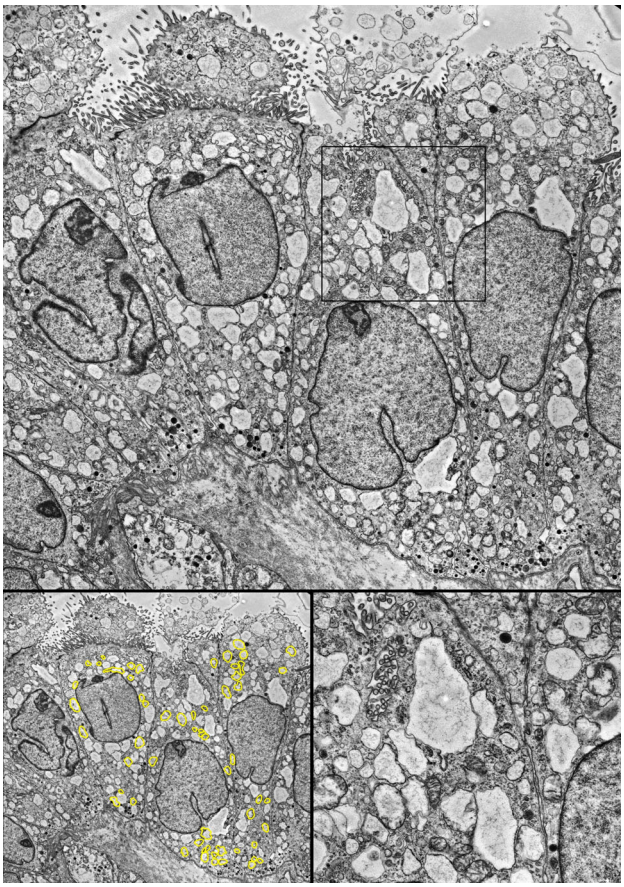

Figure 3. Cell organelle ultrastructure in classic PTC. Upper part: overview showing endoplasmic reticulum and vacuoles occupying most of the cytoplasm (case C4). Lower left: same image as above with mitochondrial mapping (yellow overlay) in three adjacent tumor cells to highlight the quantity and distribution of mitochondria. Lower right: higher magnification of the inset showing only a few morphologically normal mitochondria scattered among dilated cisternae of the endoplasmic reticulum.

were homoplasmic mtDNA-encoded complex I subunit mutations (m.3389T>C/*MT-ND1*, case C2; m.10371G>A/*MT-ND3*, case C10); both tumors harbored small tall cell subpopulations. One mutation with very low heteroplasmy (m.9654A>G) affecting the *MT-CO3* gene encoding a complex IV subunit was found in the third PTC (case C11); this last case did not have any tall cell subpopulation.

Figure 1. Histologic appearance and immunohistochemical features of PTC-TCV and cPTC. PTC-TCV (A) and classic papillary carcinoma cPTC (B), H&E staining. IHC for the pan-mitochondrial marker prohibitin shows high expression levels with strong, homogenous granular staining in PTC-TCV (C), but low levels of granular staining in cPTC (D). Expression of complex I NDUFS4 subunit is lost in the tumor cells of PTC-TCV, whereas it is preserved in endothelial cells that act as internal positive control (E); NDUFS4 expression is preserved in cPTC (F). The BRAF V600E mutated protein is expressed in the majority of tumor cells (IHC; BRAF V600E specific antibody, clone VE1) (G), while NDUFS4 loss is restricted to the tall cell subpopulation of the tumor (H, arrows), consistent with the hypothesis that papillary carcinomas first acquire *BRAF* V600E and then the mtDNA alterations that cause the tall cell phenotype (case T14).

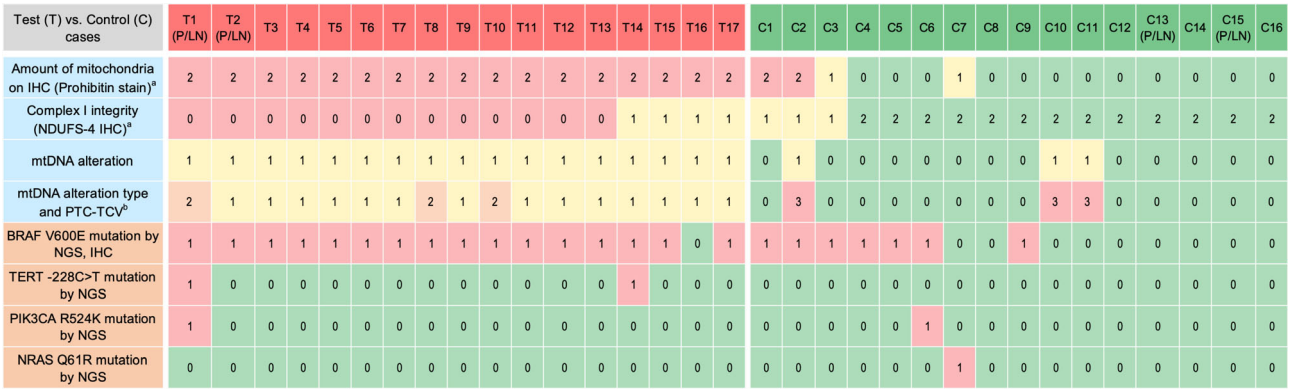

Figure 4. 'Heat map' representing the distribution of the assessed parameters among test (PTC-TCV) and control (classic PTC) cases. C, control papillary carcinoma cases (classic PTC, $n = 14$; infiltrative variant PTC, $n = 2$); LN, lymph node metastasis; P, primary tumor; T, test cases. [a]IHC. Prohibitin expression: 0, low; 1, intermediate; 2, high; NDUFS4 expression: 0, lost; 1, partially lost; 2, preserved. [b]Relationship between mtDNA alteration type and PTC-TCV histotype: 0, no mtDNA alterations and no PTC-TCV; 1, mtDNA alterations in genes encoding complex I subunits and PTC-TCV; 2, mtDNA alterations in genes not encoding complex I subunits and PTC-TCV; 3, mtDNA alterations (regardless of the mtDNA gene affected), but no PTC-TCV. Mutations in mtDNA genes and in nuclear genes: 0, absent; 1, present.

Table 2. *BRAF* V600E mutation, mtDNA mutation, and complex I integrity in PTC-TCV and control papillary carcinomas.

			Statistical significance of the difference, *p*	
Parameter	PTC-TCV ($n = 17$)	PTC control group ($n = 16$)	Uncorr.	FWER-corr.
BRAF V600E, *n* (%)	16 (94%)	7 (44%)	**0.002**	**0.002**
mtDNA mutation, *n* (%)	17 (100%)	3 (19%)	**<0.00001**	**0.00003**
Mitochondrial quantity (IHC, prohibitin stain), *n* (%)				
Low	0	12 (75%)		
Intermediate	0	2 (12.5%)		
High	17 (100%)	2 (12.5%)	**<0.00001**	**0.00003**
Complex I immunoreactivity (IHC, NDUFS4 stain), *n* (%)				
Completely lost	13 (76%)	0		
Partially lost	4 (24%)	3 (19%)		
Preserved	0	13 (81%)	**<0.00001**	**0.00003**

Bold font indicates *P* values that are statistically significant.
FWER-corr., family-wise error rate correction; Uncorr.: uncorrected.

Table 3. mtDNA mutation and complex I integrity in PTC with and without *BRAF* V600E mutation.

	BRAF status		Statistical significance of the difference, *p*	
Parameter	WT ($n = 10$)	V600E ($n = 23$)	Uncorr.	FWER-Corr.
mtDNA mutation, *n* (%)	3 (30%)	17 (74%)	**0.026**	**0.026**
Mitochondrial quantity (IHC, prohibitin stain), *n* (%)				
Low	8 (80%)	4 (17%)		
Intermediate	1 (10%)	1 (4%)		
High	1 (10%)	18 (78%)	**0.001**	**0.002**
Complex I immunoreactivity (IHC, NDUFS4 stain), *n* (%)				
Completely lost	0	13 (57%)		
Partially lost	1 (10%)	6 (26%)		
Preserved	9 (90%)	4 (17%)	**0.0004**	**0.0012**

Bold font indicates *P* values that are statistically significant.
FWER-corr., family-wise error rate correction; Uncorr., uncorrected; WT, wild type.

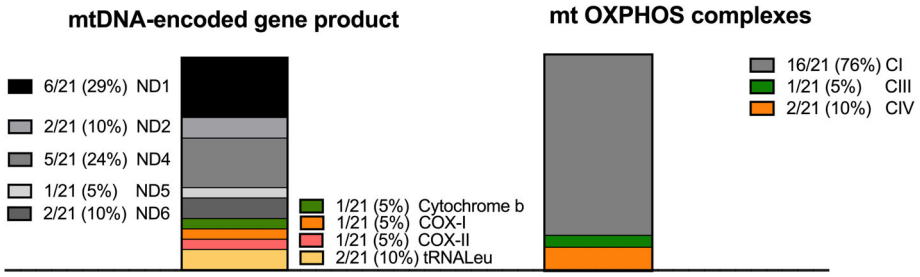

Figure 5. Distribution of mtDNA mutations in papillary carcinoma TCV. Distribution according to the mtDNA-encoded gene products (left) and according to OXPHOS mitochondrial complexes (right). Number of mtDNA mutations and percentage of the total number of mtDNA mutations identified (%). C, OXPHOS complex; COX, complex IV subunits encoded by *MT-CO* genes; ND, complex I subunits encoded by *MT-ND* genes; tRNALeu, mitochondrial transfer RNA for leucine encoded by the *MT-TL1* gene.

Papillary carcinoma TCV shows loss of OXPHOS complex I integrity by IHC

The structural stability of the respiratory complex I was evaluated by comparing the relative immunohistochemical expression of the prohibitin pan-mitochondrial marker with the nuclear DNA-encoded NDUFS4 complex I subunit. Results are illustrated in Figure 1C–F and reported in Table 2, Figure 4, and supplementary material, Table S2. PTC-TCV showed extensive granular prohibitin expression consistent with large numbers of mitochondria in neoplastic cells (Table 2 and Figure 1C; see also TEM, Figure 2). PTC control cases showed low-level granular prohibitin expression consistent with a limited number of mitochondria in neoplastic cells (Table 2 and Figure 1D; see also TEM, Figure 3). PTC-TCV showed immunohistochemical loss of NDUFS4 complex I subunit consistent with lack of complex I integrity (Table 2 and Figure 1E). Preserved NDUFS4 complex I subunit expression is consistent with proper assembly of complex I in cPTC (Table 2 and Figure 1F). Immunohistochemical results of the four cases where both the primary tumor and lymph node metastases were analyzed were concordant for each sample pair: in two PTC-TCV cases, IHC was consistent with loss of complex I integrity, in two cPTC it was consistent with proper assembly of complex I (Figure 4 and supplementary material, Table S2). Partial NDUFS4 complex I subunit loss was observed in 4 of 17 (24%) PTC-TCV and in 3 of 16 (19%) cPTC (Table 2, Figure 4, and supplementary material, Table S2). Loss (partial or complete) of complex I integrity evaluated immunohistochemically was strongly associated with PTC-TCV: it occurred in all 17 PTC-TCVs, while only partial NDUFS4 complex I subunit loss was found in 3 of 16 cPTCs ($p < 0.0001$) (Table 2, Figure 4, and supplementary material, Table S2).

mtDNA alterations correlate with loss of OXPHOS complex I integrity in papillary carcinoma TCV

Comparison of mtDNA mutations with loss of complex I assembly evaluated immunohistochemically in PTC-TCV and cPTC is reported in Table 2, Figure 4, and supplementary material, Table S2. mtDNA alterations were statistically associated with lack of complex I assembly: they were identified in 18 of 20 cases with loss (partial or complete) of complex I integrity; conversely, lack of mtDNA alterations and proper assembly of complex I occurred in 11 of 13 cases ($p < 0.0001$) (Figure 4 and supplementary material, Table S2). Among the 33 PTC cases analyzed, 9 tumors carrying nearly homoplasmic mtDNA mutations pathogenic for the mtDNA-encoded gene product in the *MT-ND* genes encoding complex I subunits showed complete loss of complex I integrity: all tumors were PTC-TCV. This is fully consistent with *in silico* data showing the disassembling potential of mtDNA mutations in PTC-TCV (Figure 4 and supplementary material, Table S2). Of the remaining eight PTC-TCV, homoplasmic/highly heteroplasmic mtDNA mutations in the *MT-ND* genes, pathogenic for the mtDNA-encoded complex I subunits, were associated with partial loss of complex I integrity restricted by IHC to a variable proportion of the population of tall cells within the tumor in four cases (Figure 4 and supplementary material, Table S2). In one additional PTC-TCV with *MT-ND1* mutation scored 'likely polymorphic' *in silico* by the bioinformatics tools (ND1 mutation-'likely polymorphic', case T2), complete NDUFS4 immunohistochemical loss in the tumor cells was consistent with *in vivo* lack of complex I integrity (Figure 4 and supplementary material, Table S2). Three further PTC-TCVs showed mtDNA mutation in genes other than the *MT-ND* genes encoding for complex I subunits as single

alterations (cases T1, T8, and T10) (Figure 4 and supplementary material, Table S2): one case (T10) carried the pathogenic m.14864G>A affecting *MT-CYB* which encodes for cytochrome *b* (Cyt *b*), a subunit of complex III (CIII); the second case (T1) carried the pathogenic m.3244G>A in *MT-TL1* (the mitochondrially encoded gene for the $tRNA^{Leu}$ transfer RNA); and the third case (T8) also carried the m.3239G>A in *MT-TL1* scored *in silico* as 'likely polymorphic'. The apparent discordance between mtDNA mutation in genes other than the *MT-ND* genes and the complete loss of complex I integrity (immunohistochemical absence of NDUFS4 in tumor cells) in the PTC-TCVs with altered *MT-CYB* can be explained by a combined CI/CIII deficiency induced by the mutation, especially considering how critical Cyt b, encoded by *MT-CYB*, is for CIII assembly [44,45]. In the two PTC-TCVs with altered *MT-TL1*, there was reduced ability of the tumor to synthesize mitochondrial proteins due to mutation of $tRNA^{Leu}$, as confirmed by the lack of expression of the mtDNA-encoded complex IV COX-I subunit demonstrated by IHC (data not shown). Alterations of mtDNA were found in three cPTCs (Figure 4 and supplementary material, Table S2). In one case (C11), there was a mutation (m.9654A>G) affecting the *MT-CO3* gene encoding a complex IV subunit which is not expected to affect complex I integrity, as confirmed by preserved immunohistochemical NDUFS4 reactivity. In two additional cPTCs, there were homoplasmic mtDNA-encoded complex I subunit mutations (m.3389T>C/*MT-ND1*, case C2; m.10371G>A/*MT-ND3*, case C10) pathogenic *in silico* for the encoded molecule. In the case with m.3389T>C/*MT-ND1* (case C2), there was partial loss of NDUFS4, but the preservation of NDUFS4 by IHC in most of the tumor cells of both cases was more in line with proper assembly of complex I *in vivo*. Interestingly, a small proportion of neoplastic cells with tall cell morphology (5–10% of the sample analyzed) was present in both tumors.

mtDNA alterations and *BRAF* V600E mutation

The relationship of *BRAF* V600E with mtDNA mutations and complex I assembly evaluated immunohistochemically is reported in Table 3, Figure 4, and supplementary material, Table S2. *BRAF* V600E is statistically associated with both mtDNA mutations and loss of complex I integrity (Table 3). BRAF V600E was identified in the majority of neoplastic cells in both PTC-TCV and cPTC. In four *BRAF* V600E mutated cases with pathogenic mtDNA mutations in *MT-ND* genes encoding complex I subunits (three PTC-TCV: T14, T15, T17; one cPTC: C2), loss of NDUSF4 expression was identified in a subpopulation of neoplastic cells, all of which showed tall cell features (Figure 1G,H, Figure 4, and supplementary material, Table S2). In these four PTCs, *BRAF* V600E was present in virtually all neoplastic cells as demonstrated by mutated allele frequencies of approximately 50% (43–61%) and diffuse immunohistochemical BRAF V600E reactivity of tumor cells. The lack of NDUSF4 expression restricted to the tall cell subpopulation of the tumors (Figure 1G,H) is consistent with the hypothesis that papillary carcinomas first acquire *BRAF* V600E and, by successively acquiring mtDNA alterations pathogenic for the encoded complex I subunits, develop the tall cell phenotype.

Discussion

In this study, we demonstrate that PTV-TCV is characterized by the accumulation of mitochondria with defective OXPHOS components due to homoplasmic/highly heteroplasmic somatic mtDNA mutations. These mutations typically affect OXPHOS complex I and underlie the oncocytic phenotype of tumors in the thyroid as well as in other organs [25–32]. The deep analogy between PTC-TCV and oncocytic tumors is reflected in the extent to which mitochondria accumulate with the resulting cytoplasmic enlargement and eosinophilia causing the 'tall cell phenomenon', and in the immunohistochemical loss of complex I integrity demonstrated by the strong, homogenous mitochondrial prohibitin stain associated with loss of NDUFS4 expression.

While oncocytes are traditionally regarded as cells in which the accumulation of mitochondria is most extreme, resulting in complete loss of cell polarity, 'tall cells' are considered mitochondria-rich cells [22,23]. Yet the tall cells of PTC-TCV – while maintaining cell polarity – share with oncocytes complete replacement of their cytoplasm by mitochondria, an event similar to that described for the 'polarized oncocytes' reported by Tsybrovskyy and Rössmann-Tsybrovskyy [46]. It is important to recognize that the degree of mitochondria accumulation represents a spectrum [23], with variation both in the extent to which mitochondria accumulate within a given cell (related to the heteroplasmy level of mtDNA alterations within the cell) and in the proportion of cells with mitochondrial accumulation within a given tumor (related to the selective advantage that cells with defective mitochondria have within the tumor microenvironment) [12,18,23]. The existence of this spectrum is well known to practicing pathologists and has been clearly outlined at the ultrastructural level in the

1980s by Sobrinho-Simões *et al* [24]. This spectrum fully explains why the diagnosis of PTC-TCV is inconsistently made by pathologists [21], in spite of the importance of correctly recognizing this tumor type given its postulated impact on prognosis [19,20].

Homoplasmic/highly heteroplasmic mtDNA mutations were identified in all PTC-TCVs. Nearly all were predicted to be pathogenic for the encoded protein *in silico*. The only two mutations that did not score as pathogenic (they were classified as 'likely polymorphic' *in silico*) resulted in a loss of complex I by IHC indicating that they were also able to produce a phenotypic effect. Mutations of mtDNA pathogenic for the encoded molecules and occurring in homoplasmic/highly heteroplasmic mtDNA showed an excellent correlation with loss of complex I integrity demonstrated by IHC as loss of NDUFS4 expression. The three PTC-TCVs where pathogenic mtDNA mutations occurred in genes not encoding complex I subunits also showed NDUFS4 loss: in one, the mutation affected *MT-CYB* encoding for Cyt b (a subunit of complex III) and in two the mutation affected *MT-TL1* encoding the mitochondrial $tRNA^{Leu}$. In the two *MT-TL1*-mutated PTC-TCVs, there was a generalized reduced ability of the tumor to synthesize mitochondrial proteins as indicated by the concurrent immunohistochemical loss of both NDUFS4 and of the mtDNA-encoded complex IV COX-I subunit, as reported in mitochondriopathies where these mutations occur in the germline [41]. The lack of complex I integrity in the *MT-CYB*-mutated PTC-TCV can be explained by the necessity of proper assembly of complex III for complex I maturation [44,45].

Our data support the observations of Zimmermann *et al* showing how, in oncocytic tumors, NDUFS4 is a marker reliably expressed when complex I is intact and, conversely, universally lost with complex I defects [42]. Our data indicate that immunohistochemical loss of NDUFS4 is a sensitive surrogate marker of OXPHOS disruption in general terms, regardless of the specific type of the underlying genetic alteration, as it is also lost in tumors with mutations in OXPHOS components other than complex I. The facts that expression of the NDUFS4 subunit depends highly on the presence of the preassembled complex I, that the stability of the entire complex I depends on other OXPHOS components (especially complex III) [44] and, furthermore, that complexes I, III, and IV demonstrate tight spatial and functional integration by forming 'supercomplexes' or 'respirasomes' [45] are reasonable explanations for this phenomenon. Thus, IHC for prohibitin – a mitochondrial protein that is highly evolutionarily conserved and not directly related to OXPHOS or energy metabolism [40] – as a pan-mitochondrial marker, and for NDUFS4 as a sensitive OXPHOS marker, can be used to assess OXPHOS integrity in general and to specifically identify tall cells in routine surgical specimens. Interestingly, adverse clinicopathologic features have been associated with cases showing tall cell morphology at the H&E level in ≥30% of the tumors in PTC, including microcarcinomas [12,47]. Immunohistochemical OXPHOS assessment with prohibitin and NDUFS4 should help standardize the diagnosis of the TCV and therefore to clarify its clinicopathologic features and ultimately the impact of this diagnosis on patient outcome.

One important difference between PTC-TCV and oncocytic tumors is the almost universal occurrence of *BRAF* V600E mutation in PTC-TCV and its absence in oncocytic tumors. *BRAF* V600E mutation was found in all but one of our PTC-TCV, confirming the very high prevalence of this mutation in this tumor type to the point of being one of its defining molecular features [33]. Conversely, *BRAF* V600E mutation hardly ever occurs in conventional oncocytic tumors [48]. Interestingly, the widespread loss of heterozygosity arising from haploidization and copy number neutral uniparental disomy of oncocytic thyroid tumors [48] has not been reported in PTC-TCV [33,34]. Our data indicate that in PTC-TCV the *BRAF* V600E mutation occurs before the development of mtDNA alterations, as shown in cases where pathogenic mutations in *MT-ND* genes and loss of complex I integrity were limited to subpopulations of neoplastic tall cells within tumors with high *BRAF* V600E mutated allelic fraction and widespread immunohistochemical expression of the mutated protein. This finding and the tight association between homoplasmic/highly heteroplasmic mtDNA mutations and PTC-TCV raise the question of how BRAF V600E may predispose to the development of pathogenic mtDNA alterations. Several studies have shown that, in BRAF V600E-driven malignancies, OXPHOS gene programs and mitochondrial biogenesis as well as mitophagy – the intracellular process of selective degradation of mitochondria by autophagy – are inhibited [49–51]. Specifically, in thyroid cancer cells, BRAF V600E mutation alters the HIF1α-MYC-PGC-1β axis, causing mitochondrial respiration to be inhibited and aerobic glycolysis to be enhanced (akin to the Warburg effect) [49]. It is possible that this context of decreased OXPHOS function and mitochondrial turnover creates a favorable condition for mtDNA mutations to accumulate and to fix at homoplasmic/highly heteroplasmic levels, resulting in the tall cell phenotype. Figure 6 summarizes PTC-TCV molecular alterations and their impact on neoplastic cell metabolism.

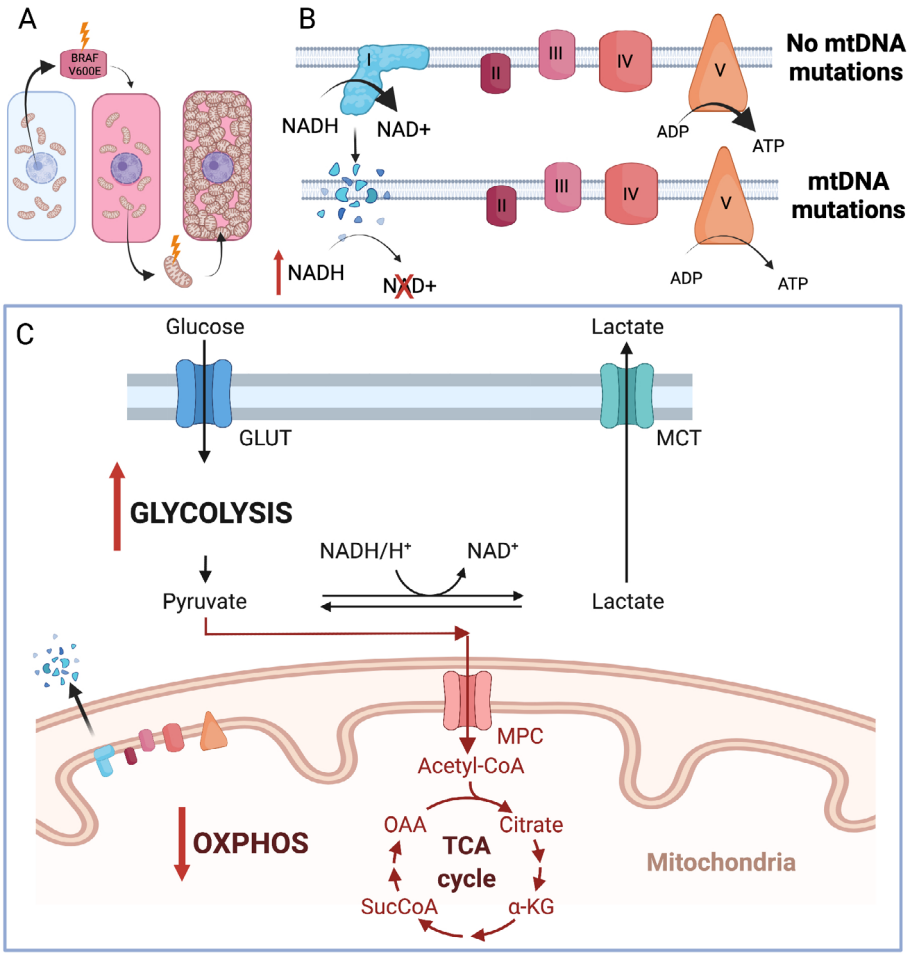

Figure 6. PTC-TCV molecular alterations and their impact on neoplastic cell metabolism. (A) PTCs first acquire *BRAF* V600E and then mtDNA mutations leading to OXPHOS impairment and compensatory increase of mitochondria. (B) Mutations affecting mtDNA genes – typically the *MT-ND* genes encoding ND complex I subunits that anchor the molecule to the inner mitochondrial membrane or less commonly other mtDNA genes – cause loss of OXPHOS complex I assembly. (C) Loss of complex I integrity impairs OXPHOS, leading to increased glycolysis and (A) compensatory increase of deficient mitochondria. α-KG: α-ketoglutaric acid; Acetyl-CoA, acetyl coenzyme A; ADP, adenosine diphosphate; ATP, adenosine triphosphate; GLUT, glucose transporter; MCT, monocarboxylate transporter; MPC, mitochondrial pyruvate carrier; NAD+, nicotinamide adenine dinucleotide+; NADH, nicotinamide adenine dinucleotide hydrogen; OAA, oxaloacetic acid; SucCoA, succinyl-coenzyme A; TCA, tricarboxylic acid cycle. Figure created with BioRender.com.

In spite of this important difference, there are surprising similarities between PTC-TCV and oncocytic carcinomas of follicular cells, indicating that the shared mitochondrial alterations are also reflected in similar clinicopathologic features. In both instances, patients are older at the time of diagnosis, both tumor types have a larger size and more frequent extrathyroidal extension at the time of presentation, and both frequently manifest with disease in the neck (sometimes bulky) compared with conventional PTC and non-oncocytic follicular carcinomas, respectively [23,52]. The most clinically relevant analogy between PTC-TCV and thyroid oncocytic carcinomas is that, while relatively uncommon, they are both overrepresented among the thyroid cancers of follicular cells with unfavorable outcome. PTC-TCV represents approximately 10–15% of all PTCs in most series [16], but together with oncocytic carcinoma constitutes 55% of the tumors that are refractory to RAI treatment without exhibiting high grade or anaplastic histology [53]. These same tumor types make up approximately 70% of the thyroid carcinomas that are fatal to the patient, in the absence of the unfavorable histologic features mentioned above (high grade or anaplastic histology) [9]. A likely explanation is that, in both PTC-TCV and thyroid oncocytic carcinomas, impairment of OXPHOS and energy metabolism interfere with the uptake of iodide by

the tumor cells making them resistant to RAI ablation. In the case of PTC-TCV, the BRAF V600E mutation, by independently inducing a less differentiated functional phenotype with lower thyroid differentiation score [33], may further hinder iodide uptake.

In our series, PTC-TCV developed in older patients, tended to be larger, and showed greater extrathyroidal extension. However, the small number of cases and the limited follow-up preclude the relevance of clinicopathologic analysis.

The quest to identify the cause of the 'tall cell phenomenon' is old [54]. Here, we demonstrate that PTC-TCV carries the same mitochondrial OXPHOS defects of oncocytic tumors that – as in the case of oncocytic tumors – result in loss of complex I integrity and in an extreme degree of mitochondria accumulation, that underlie the cytoplasmic eosinophilia and the histologic features of tall cells. We also show that IHC for prohibitin, as a pan-mitochondrial marker, and for the complex I subunit NDUFS4, can be used to assess OXPHOS integrity and to thus reliably identify tall cells in routine surgical specimens.

Acknowledgement

MDL was supported by the Associazione Italiana per la Ricerca sul Cancro (AIRC) 'Bruna Martelli' Fellowship.

Author contributions statement

OT, MSS and GT designed the study and produced the pathology data. DH, LI and SH produced the clinical data. OT, DdB, LC, CF and MDL performed the experiments. OT, GT, DdB, LC, CF, VC, GG and MDL analyzed the data and contributed to data interpretation. GT, OT and MDL wrote the manuscript with input from all authors.

References

1. Hawk WA, Hazard JB. The many appearances of papillary carcinoma of the thyroid. *Cleve Clin Q* 1976; **43:** 207–215.
2. Bongers PJ, Kluijfhout WP, Verzijl R, *et al*. Papillary thyroid cancers with focal tall cell change are as aggressive as tall cell variants and should not be considered as low-risk disease. *Ann Surg Oncol* 2019; **26:** 2533–2539.
3. Ho AS, Luu M, Barrios L, *et al*. Incidence and mortality risk spectrum across aggressive variants of papillary thyroid carcinoma. *JAMA Oncol* 2020; **6:** 706–713.
4. Ito Y, Hirokawa M, Miyauchi A, *et al*. Prognostic significance of the proportion of tall cell components in papillary thyroid carcinoma. *World J Surg* 2017; **41:** 742–747.
5. Johnson TL, Lloyd RV, Thompson NW, *et al*. Prognostic implications of the tall cell variant of papillary thyroid carcinoma. *Am J Surg Pathol* 1988; **12:** 22–27.
6. Kazaure HS, Roman SA, Sosa JA. Aggressive variants of papillary thyroid cancer: incidence, characteristics and predictors of survival among 43,738 patients. *Ann Surg Oncol* 2012; **19:** 1874–1880.
7. Morris LG, Shaha AR, Tuttle RM, *et al*. Tall-cell variant of papillary thyroid carcinoma: a matched-pair analysis of survival. *Thyroid* 2010; **20:** 153–158.
8. Shi X, Liu R, Basolo F, *et al*. Differential clinicopathological risk and prognosis of major papillary thyroid cancer variants. *J Clin Endocrinol Metab* 2016; **101:** 264–274.
9. Xu B, Ibrahimpasic T, Wang L, *et al*. Clinicopathologic features of fatal non-anaplastic follicular cell-derived thyroid carcinomas. *Thyroid* 2016; **26:** 1588–1597.
10. Akslen LA, LiVolsi VA. Prognostic significance of histologic grading compared with subclassification of papillary thyroid carcinoma. *Cancer* 2000; **88:** 1902–1908.
11. Axelsson TA, Hrafnkelsson J, Olafsdottir EJ, *et al*. Tall cell variant of papillary thyroid carcinoma: a population-based study in Iceland. *Thyroid* 2015; **25:** 216–220.
12. Ganly I, Ibrahimpasic T, Rivera M, *et al*. Prognostic implications of papillary thyroid carcinoma with tall-cell features. *Thyroid* 2014; **24:** 662–670.
13. Kim Y, Roh JL, Song DE, *et al*. Risk factors for posttreatment recurrence in patients with intermediate-risk papillary thyroid carcinoma. *Am J Surg* 2020; **220:** 642–647.
14. Michels JJ, Jacques M, Henry-Amar M, *et al*. Prevalence and prognostic significance of tall cell variant of papillary thyroid carcinoma. *Hum Pathol* 2007; **38:** 212–219.
15. Prendiville S, Burman KD, Ringel MD, *et al*. Tall cell variant: an aggressive form of papillary thyroid carcinoma. *Otolaryngol Head Neck Surg* 2000; **122:** 352–357.
16. Regalbuto C, Malandrino P, Frasca F, *et al*. The tall cell variant of papillary thyroid carcinoma: clinical and pathological features and outcomes. *J Endocrinol Invest* 2013; **36:** 249–254.
17. Song E, Jeon MJ, Oh HS, *et al*. Do aggressive variants of papillary thyroid carcinoma have worse clinical outcome than classic papillary thyroid carcinoma? *Eur J Endocrinol* 2018; **179:** 135–142.
18. Wong KS, Higgins SE, Marqusee E, *et al*. Tall cell variant of papillary thyroid carcinoma: impact of change in WHO definition and molecular analysis. *Endocr Pathol* 2019; **30:** 43–48.
19. Filetti S, Durante C, Hartl D, *et al*. Thyroid cancer: ESMO Clinical Practice Guidelines for diagnosis, treatment and follow-up†. *Ann Oncol* 2019; **30:** 1856–1883.
20. Haugen BR. 2015 American Thyroid Association management guidelines for adult patients with thyroid nodules and differentiated thyroid cancer: what is new and what has changed? *Cancer* 2017; **123:** 372–381.
21. Hernandez-Prera JC, Machado RA, Asa SL, *et al*. Pathologic reporting of tall-cell variant of papillary thyroid cancer: have we reached a consensus? *Thyroid* 2017; **27:** 1498–1504.

22. Lloyd RV, Osamura RY, Klöppel G, *et al*. *WHO Classification of Tumours of Endocrine Organs*. International Agency for Research on Cancer: Lyon, 2017; 81–91.
23. Rosai J, DeLellis RA, Carcangiu ML, *et al*. *Tumors of the Thyroid and Parathyroid Glands*. ARP Press: Silver Spring, 2014; 199–220.
24. Sobrinho-Simões MA, Nesland JM, Holm R, *et al*. Hürthle cell and mitochondrion-rich papillary carcinomas of the thyroid gland: an ultrastructural and immunocytochemical study. *Ultrastruct Pathol* 1985; **8:** 131–142.
25. Bonora E, Porcelli AM, Gasparre G, *et al*. Defective oxidative phosphorylation in thyroid oncocytic carcinoma is associated with pathogenic mitochondrial DNA mutations affecting complexes I and III. *Cancer Res* 2006; **66:** 6087–6096.
26. Gasparre G, Porcelli AM, Bonora E, *et al*. Disruptive mitochondrial DNA mutations in complex I subunits are markers of oncocytic phenotype in thyroid tumors. *Proc Natl Acad Sci U S A* 2007; **104:** 9001–9006.
27. Gopal RK, Kübler K, Calvo SE, *et al*. Widespread chromosomal losses and mitochondrial DNA alterations as genetic drivers in Hürthle cell carcinoma. *Cancer Cell* 2018; **34:** 242–255.e5.
28. Gasparre G, Hervouet E, de Laplanche E, *et al*. Clonal expansion of mutated mitochondrial DNA is associated with tumor formation and complex I deficiency in the benign renal oncocytoma. *Hum Mol Genet* 2008; **17:** 986–995.
29. Gopal RK, Calvo SE, Shih AR, *et al*. Early loss of mitochondrial complex I and rewiring of glutathione metabolism in renal oncocytoma. *Proc Natl Acad Sci U S A* 2018; **115:** E6283–E6290.
30. Mayr JA, Meierhofer D, Zimmermann F, *et al*. Loss of complex I due to mitochondrial DNA mutations in renal oncocytoma. *Clin Cancer Res* 2008; **14:** 2270–2275.
31. Müller-Höcker J, Schäfer S, Krebs S, *et al*. Oxyphil cell metaplasia in the parathyroids is characterized by somatic mitochondrial DNA mutations in NADH dehydrogenase genes and cytochrome c oxidase activity-impairing genes. *Am J Pathol* 2014; **184:** 2922–2935.
32. Porcelli AM, Ghelli A, Ceccarelli C, *et al*. The genetic and metabolic signature of oncocytic transformation implicates HIF1alpha destabilization. *Hum Mol Genet* 2010; **19:** 1019–1032.
33. Cancer Genome Atlas Research Network. Integrated genomic characterization of papillary thyroid carcinoma. *Cell* 2014; **159:** 676–690.
34. Cavadas B, Pereira JB, Correia M, *et al*. Genomic and transcriptomic characterization of the mitochondrial-rich oncocytic phenotype on a thyroid carcinoma background. *Mitochondrion* 2019; **46:** 123–133.
35. de Biase D, Acquaviva G, Visani M, *et al*. Molecular diagnostic of solid tumor using a next generation sequencing custom-designed multi-gene panel. *Diagnostics (Basel)* 2020; **10:** 250.
36. Kurelac I, MacKay A, Lambros MB, *et al*. Somatic complex I disruptive mitochondrial DNA mutations are modifiers of tumorigenesis that correlate with low genomic instability in pituitary adenomas. *Hum Mol Genet* 2013; **22:** 226–238.
37. Calabrese C, Simone D, Diroma MA, *et al*. MToolBox: a highly automated pipeline for heteroplasmy annotation and prioritization analysis of human mitochondrial variants in high-throughput sequencing. *Bioinformatics* 2014; **30:** 3115–3117.
38. Preste R, Vitale O, Clima R, *et al*. HmtVar: a new resource for human mitochondrial variations and pathogenicity data. *Nucleic Acids Res* 2019; **47:** D1202–D1210.
39. Del Dotto V, Ullah F, Di Meo I, *et al*. SSBP1 mutations cause mtDNA depletion underlying a complex optic atrophy disorder. *J Clin Invest* 2020; **130:** 108–125.
40. Hernando-Rodríguez B, Artal-Sanz M. Mitochondrial quality control mechanisms and the PHB (prohibitin) complex. *Cells* 2018; **7:** 238.
41. Sasarman F, Antonicka H, Shoubridge EA. The A3243G tRNALeu(UUR) MELAS mutation causes amino acid misincorporation and a combined respiratory chain assembly defect partially suppressed by overexpression of EFTu and EFG2. *Hum Mol Genet* 2008; **17:** 3697–3707.
42. Zimmermann FA, Mayr JA, Neureiter D, *et al*. Lack of complex I is associated with oncocytic thyroid tumours. *Br J Cancer* 2009; **100:** 1434–1437.
43. Holm S. A simple sequentially rejective multiple test procedure. *Scand J Stat* 1979; **6:** 65–70.
44. Acín-Pérez R, Bayona-Bafaluy MP, Fernández-Silva P, *et al*. Respiratory complex III is required to maintain complex I in mammalian mitochondria. *Mol Cell* 2004; **13:** 805–815.
45. Protasoni M, Pérez-Pérez R, Lobo-Jarne T, *et al*. Respiratory supercomplexes act as a platform for complex III-mediated maturation of human mitochondrial complexes I and IV. *EMBO J* 2020; **39:** e102817.
46. Tsybrovskyy O, Rössmann-Tsybrovskyy M. Oncocytic versus mitochondrion-rich follicular thyroid tumours: should we make a difference? *Histopathology* 2009; **55:** 665–682.
47. Tallini G, de Biase D, Durante C, *et al*. BRAF V600E and risk stratification of thyroid microcarcinoma: a multicenter pathological and clinical study. *Mod Pathol* 2015; **28:** 1343–1359.
48. Ganly I, McFadden DG. Short review: genomic alterations in Hürthle cell carcinoma. *Thyroid* 2019; **29:** 471–479.
49. Gao Y, Yang F, Yang XA, *et al*. Mitochondrial metabolism is inhibited by the HIF1alpha-MYC-PGC-1beta axis in BRAF V600E thyroid cancer. *FEBS J* 2019; **286:** 1420–1436.
50. Haq R, Shoag J, Andreu-Perez P, *et al*. Oncogenic BRAF regulates oxidative metabolism via PGC1alpha and MITF. *Cancer Cell* 2013; **23:** 302–315.
51. Strohecker AM, White E. Targeting mitochondrial metabolism by inhibiting autophagy in BRAF-driven cancers. *Cancer Discov* 2014; **4:** 766–772.
52. Cracolici V, Kadri S, Ritterhouse LL, *et al*. Clinicopathologic and molecular features of metastatic follicular thyroid carcinoma in patients presenting with a thyroid nodule versus a distant metastasis. *Am J Surg Pathol* 2019; **43:** 514–522.
53. Rivera M, Ghossein RA, Schoder H, *et al*. Histopathologic characterization of radioactive iodine-refractory fluorodeoxyglucose-positron emission tomography-positive thyroid carcinoma. *Cancer* 2008; **113:** 48–56.

54. Flint A, Davenport RD, Lloyd RV. The tall cell variant of papillary carcinoma of the thyroid gland. Comparison with the common form of papillary carcinoma by DNA and morphometric analysis. *Arch Pathol Lab Med* 1991; **115:** 169–171.

55. Diroma MA, Lubisco P, Attimonelli M. A comprehensive collection of annotations to interpret sequence variation in human mitochondrial transfer RNAs. *BMC Bioinformatics* 2016; **17**(Suppl 12)**:** 338.

Reference 55 is cited only in the supplementary material.

SUPPLEMENTARY MATERIAL ONLINE

Supplementary materials and methods

Table S1. Antibody clones and immunostaining protocols

Table S2. Mitochondrial alterations in tall cell papillary carcinoma and papillary thyroid carcinoma control cases